THERMAL BLOOMING OF REPETITIVELY PULSED OPTICAL RADIATION IN A GAS FLOW

V.V. Vorob'ev, M.N. Kogan, A.N. Kucherov and E.V. Ustinov

Moscow Institute of Atmospheric Physics
Received September 19, 1988

We conduct numerical investigations of thermal blooming of an optical pulse train in an absorbing gas medium moving transverse to the beam at subsonic, transonic and supersonic velocities. In the subsonic and supersonic gas dynamics regimes, computer simulations are performed up to the point when a quasistationary blooming mode has been established. We show that during stabilization, the laser peak intensity can considerably exceed both its initial value and the value for the stabilized quasistat ionary mode. We investigated the effect of2 the pulse repetition rate on quasistationary blooming mode.

The various and sundry investigations of the thermal blooming effects[1–3] have scarcely touched upon the thermal blooming of the repetitively pulsed radiation in the transverse flow of a gaseous substance. One can find only a few such papers[4–6], and in those, propagation effects in a gas flow with a relatively small transverse velocity (i.e. the convective gas dynamic case) are described.

This paper considers the thermal blooming of a repetitively pulsed beam in the subsonic and supersonic gas dynamic flows, including the quasistationary limit in which perturbations of the medium become periodic.

Under the assumptions of a very small viscosity and thermal conductivity the gas dynamics equations using physical variables are as follows:

$$\frac{d}{dt}\rho + \rho(\nabla,\mathbf{V}) = 0\ ; \quad \frac{d}{dt} = \frac{\partial}{\partial t} + \left(\mathbf{V},\vec{\nabla}\right)\ ;$$

$$\nabla = i\frac{\partial}{\partial x} + j\frac{\partial}{\partial y}\ ;$$

$$\rho\frac{d\mathbf{V}}{dt} + \nabla P = 0\ ; \qquad (1)$$

$$\frac{d}{dt}\left[\ln\left(\frac{P}{\rho^{æ}}\right)\right] = \frac{æ-1}{P}\rho k I_{*} I(x,y,z,t).$$

Here t is the time, x, y, z are the coordinates (z is the axis along the propagation direction and x is the axis along the direction of the gas flow), ρ is the density, P is the pressure, $\mathbf{V}$ is the gas flow velocity, κ is the adiabatic exponent, i and j are the unit vectors along the x and y axes, k is the absorption coefficient per unit mass ($\alpha = k\rho$ is the volume absorption coefficient), I_* is the characteristic beam intensity, I is the dimensionless distribution function.

Since the laser beam cross-section a is considerably less than the propagation length L, the gas flow is assumed to be two-dimensional. The gas dynamic variables depend on z as a parameter. Let us introduce into consideration the pulse duration τ_1 and the pulse repetition period τ_2. Assume that $\tau_1 \ll \tau_2 \sim \tau_v$, where $\tau_v = a/V_0$ is the typical gas dynamic time and V_0 is the initial gas flow velocity. Let a be the laser–beam radius (geometrical for a uniform irradiance distribution or exponential for a Gaussian beam). For the typical intensity, we take the time-averaged (over a pulse) and space-averaged beam intensity $I_* = E_1/(\pi a^2\tau_1)$, where

$$E_1 = \int_0^{\tau_1} dt \iint_{-\infty}^{+\infty} I_{*} I(x,y,z,t)\, dxdy$$

is the energy of a single pulse. If the pulse has a rectangular temporal profile, the distribution function will be

$$I(x,y,z,t) = I_1(x,y,z),$$

for $0 \le t/\tau_1 \le 1$, where I_1 is a dimensionless function of coordinates.

The absorbed energy is generally small in comparison with the gas enthalpy, so the gas dynamic perturbations are also small. Thus the linearization of the gas dynamic equations is possible. For a single pulse and for a time interval of about τ_1, the following expansions and solutions for the dimensionless linearized equations of gas dynamics (1) can easily be obtained (note that in this case the notations used for the coordinates and the time are the same):

$$P/P_0 = 1 + æ M^2 \delta P_1 + \ldots;\ V_0 = i + \frac{\tau_1}{\tau_v}\delta \mathbf{V}_1 + \ldots;$$

$$\rho/\rho_0 = 1 + \left(\frac{\tau_1}{\tau_v}\right)^2 \delta\rho_1 + \ldots; \qquad (2)$$

$$P_1 = \frac{1}{M^2}\int_0^t I(x,y,z,t')\,dt' = \frac{t}{M^2} I_1(x,y,z);$$

$$\mathbf{V}_1 = -\frac{1}{M^2}\int_0^t \vec{\nabla} P(x,y,z,t')dt' = -\frac{t^2}{2M^2}\vec{\nabla} I_1(x,y,z); \qquad (3)$$

$$\rho_1 = -\int_0^t (\vec{\nabla}, \mathbf{V}_1(x,y,z,t'))dt' = \frac{t^3}{6M^2}\nabla^2 I_1(x,y,z).$$

Here

$$\delta = \frac{æ - 1}{æ P_0}\,\alpha\, I_* \tau_1$$

is a small parameter which characterizes the pressure perturbation scale, P_0, ρ_0, V_0 are the pressure, density and velocity of the unperturbed gas, respectively, c is the speed of sound in the latter $M = V_0/c$ is the Mach number.

It is obvious that for a time interval of about $\tau_2 \sim \tau_v$, no heating sources are involved in the energy balance equations. But pressure perturbations occur in gas (as follows from Eq. (2) the magnitudes of other gas dynamic variables are smaller), and due to acoustic wave propagation they will in turn perturb the gas itself. It is clear that the perturbation scale of the gas dynamic variables τ_2 for is equal to δ. Assume that τ_v is a characteristic time and denote the dimensionless period between pulses as $\tau = \tau_2/\tau_y \sim 1$. To justify a subsequent comparison between CW radiation and pulsed radiation, it is necessary to choose the same mean power for both the repetitively pulsed mode and the CW mode: CW mode, $\varepsilon = \frac{\kappa - 1}{\kappa P_0}\alpha I_{cw}\tau_v$ will be related as $\delta = \varepsilon\tau$.

To compare the CW and pulsed modes, we perform a series expansion over the small parameter of the gas dynamic variables, with due regard for this relation. Thus

$$\frac{P}{P_0} = 1 + æ M^2 \varepsilon P_1 + \ldots; \quad \frac{\mathbf{V}}{V_0} = 1 + \varepsilon \mathbf{V}_1;$$

$$\rho/\rho_0 = 1 + \varepsilon\rho_1 + \ldots \qquad (4)$$

Substituting Eq. (4) into Eq. (1), one obtains the following set of equations for the main terms of the gas dynamic perturbations:

$$\frac{d}{dt}\rho_1 + (\nabla, \mathbf{V}_1) = 0; \quad \frac{d}{dt} = \frac{\partial}{\partial t} + \frac{\partial}{\partial x};$$

$$\frac{d}{dt}\mathbf{V}_1 + \nabla P_1 = 0; \quad \frac{d}{dt}(M^2 P_1 - \rho_1) = 0. \qquad (5)$$

Taking into consideration Eq. (2) and Eq. (3), the initial conditions for this set of equations will be

$$\rho_1|_{t=0} = 0; \quad \nabla_1|_{t=0} = 0; \quad \rho_1|_{t=0} = \frac{\tau}{M^2} I_1(x,y,z) \qquad (6)$$

For a pulse train, the gas dynamic perturbations from any n-th pulse for the time interval τ_1 will be described by a solution similar to Eq. (3). To find the perturbations for the time interval τ, the set of equations (5) with the following initial conditions has to be solved:

$$\rho_1|_{t=t_n} = \rho_{1,n-1}(x,y,z,t_n);$$

$$\mathbf{V}_1|_{t=t_n} = \mathbf{V}_{1,n-1}(x,y,z,t_n);$$

$$P_1|_{t=t_n} = P_{1,n-1} + \frac{\tau}{M^2} I_n(x,y,z). \qquad (7)$$

Here $P_{1,n-1}$; $\rho_{1,n-1}$; $V_{1,n-1}$ designate the solutions of Eq. (5) for the $(n-1)$-th pulse.

The set of equations (5) is solved using McCormack's finite-difference technique[8] to second order in the spatial coordinates and the time. The intensity distribution function I_1 at $z = 0$ has the Gaussian shape $I_1 = \exp(-x^2 - y^2)$. The boundary conditions are specified at a relatively large distance from the heat sources (I_x, I_y = 3, 2; 4, 8; 6, 4). Extrapolation the solution from the adjacent internal grid points rather than using zero boundary conditions for ρ_1, V_1, P_1 enables us to significantly reduce the size of the computational grid. An analysis shows that even for a relatively small grid size, I_x, I_y = 3, 2, the computational errors are less than 1% at times of order $(5-7)\tau_v$ for all cases considered below: M = 0.5; 0.8; 1; 2. It is further assumed that $\tau_2 = 10^{-3}$ sec, $\tau_v = 10^{-2}$ sec/(3M) (a = 0.5 m, c = 300 m/sec), so the period τ is equal 0.3 (for M = 0.5), τ = 0.48 (for M = 0.8), τ = 0.6 (for M = 1.0) and τ = 1.2 (for M = 2.0).

The propagation of laser beams with a small divergence is described by the so-called paraxial optics equation, which may be written in terms of normalized variables (together with the initial and the boundary conditions) as

$$2F\frac{\partial u}{\partial z} + i\nabla^2 u + \left[2iF^2 N \rho_1(I_n, M) + FN_\alpha\right]u = 0 \qquad (8)$$

$$u|_{z=0} = u_0(x,y) \qquad (9)$$

$$u|_{x,\,y \;\pm\infty \longrightarrow} 0 \qquad (10)$$

Here u is the complex field function, $I_n = uu^*$ is the intensity of the n-th pulse, $F = 2\pi n_0 a^2/\lambda L$ is the Fresnel number, λ is the the wavelength, n_0 is the refractive index of the undisturbed gas, $N_\alpha = \alpha L$ is the absorption (attenuation) parameter, $N = (L/z_T)^2$ is the blooming parameter of self-influence and

$z_T = a / \sqrt{\varepsilon(n_0 - 1) / n_0}$ is the thermal blooming distance.

The characteristic path length L will be assumed to be equal to z_T, since the thermal blooming effect (at $N = 1$) is to be studied. An initially collimated Gaussian beam $u_0 = \exp\{-(x^2 + y^2)/2\}$ will be considered. To find the solution of Eq. (8), Fourier series expansion and fast Fourier transform techniques have been used.

This paper investigates the thermal blooming effects in the subsonic ($M = 0.5$, $\tau = 0.3$ and $M = 0.8$, $\tau = 0.48$) mode, the supersonic ($M = 2.0$, $\tau = 1.2$) mode, and the transonic ($M = 1.0$, $\tau = 0.6$) mode, which is the initial phase of the supersonic mode with linear perturbations.

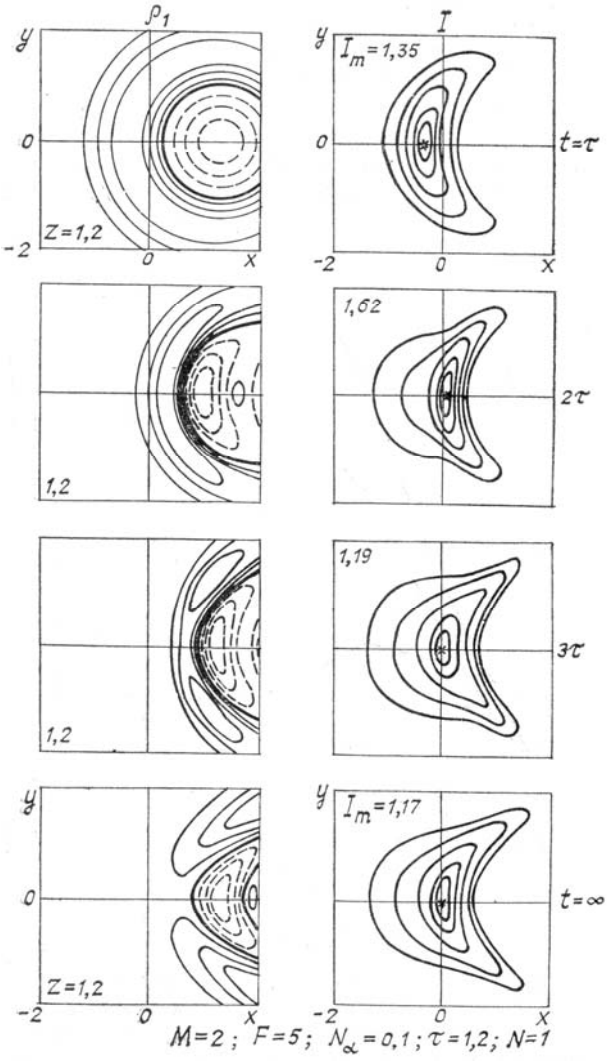

FIG. 1.

Figure 1 presents numerical results for supersonic mode ($M = 2$, $\tau = 1.2$) at times $t = \tau$, 2τ, 3τ and for the quasistationary limit which will be explained in detail below. The Fresnel number is 5, $N_\alpha = 0.1$. The constant density (left) and the constant irradiance (right) contours are shown, where the fixed irradiance levels are 0.9, 0.75, 0.5, 0.25 and 0.1 of $I_{max} = \max_{xy}\{I\}/z = \text{const}$. The position of the peak irradiance is marked by "x" and the I_{max} value is presented in the left upper corner. It can be seen that the irradiance perturbation pattern is already stabilized by the fourth pulse (the first pulse propagates through the undisturbed density field), although the density perturbation pattern is quite different from that which exists at the time $t = n\tau$, where $n \gg 1$. The fixed density levels are shown by solid curves for $\rho_1 = 0.75, 0.5, 0.25$ of ρ_{1max}, by a bold solid curve for $\rho = 0$, and by the dashed curves for $\rho_1 = 0.75, 0.5, 0.25$ of ρ_{1min}. .The development of a high density area on the side exposed to the flow after the second pulse and of two symmetrical high density areas in the Mach waves after the third pulse is clearly visible. A strong rarefaction of the gas on the opposite side of the beam results in forcing the radiation out of this area, and even for the second pulse the constant density contours are the crescent-shaped.

The dependence of the peak intensity I_{max} on the distance z along the beam for many pulses (for the supersonic mode it is valid for all pulses starting from the second one) has the same cross section ($z = \text{const}$) as the absolute maximum, which we henceforth refer to as the focal cross section. The focal length is approximately $z_f = 1.0$–1.2 for the subsonic mode ($M = 0.5$ and 0.8); it changes from $z = 1.35$ to $z_f = 1$ for the transonic flow ($M = 1$), and varies between $z_f = 1.2$ and $z_f = 1.4$ for the for the transonic flow ($M = 2$). The results shown in Fig. 1 are presented for the cross section $z_{phys} = 1.2\ z_\tau$, which is similar to the focal cross section.

Figure 2 shows the variation of I_{max} from pulse to pulse for different M numbers and fixed values of $F = 5$ and $N\alpha = 0.1$. The values of the peak intensity are presented for the thermal blooming distance $z_{phys} = z_T$. For $M = 0.5$ and $M = 2$, the peaks of intensity I_{max} are stabilized at levels close to the corresponding levels occurring in the quasistationary modes. The results are obtained for these modes by using another method which will be described below. For $M = 0.8$, the stabilization will be achieved after a slightly longer time than that shown in Fig. 2 while for $M = 1$, as expected, a continuous intensity increase is observed for all pulses, starting from the second.

For all modes under consideration except the supersonic mode, the beam is mainly defocused during the propagation of the second pulse. Similar behavior of the peak intensity (a "dive" at the initial interval $0 < t < \tau_V$, then a growth up to a certain peak value and finally the stabilization at a stationary level) was observed earlier for unstabilized thermal blooming in the case of CW radiation that was switched on instantaneously (like a "step") or linearly during the time τ_V.[10] The results were obtained for a two-dimensional (slot) beam. In this paper a comparative analysis for repetitively pulsed and unstabilized CW modes has been carried out for

subsonic (M = 0.5 and 0.8), transonic (M = 1), and supersonic (M = 2) gas flows. The analysis is based on computations for three-dimensional (circular) Gaussian beams. Assume that the CW radiation is switched on instantaneously (like a "step"). The differences in the gas dynamic equations are as follows: in Eq. (5) the heat source function $I(x,y.z)$ appears while the initial conditions (6) and (7) become equal to zero. The gas dynamic equations (5) and the paraxial equation (8) should be solved simultaneously at each time step, while for the repetitively pulsed radiation, Eq. (8) at a multiple of the pulse period.

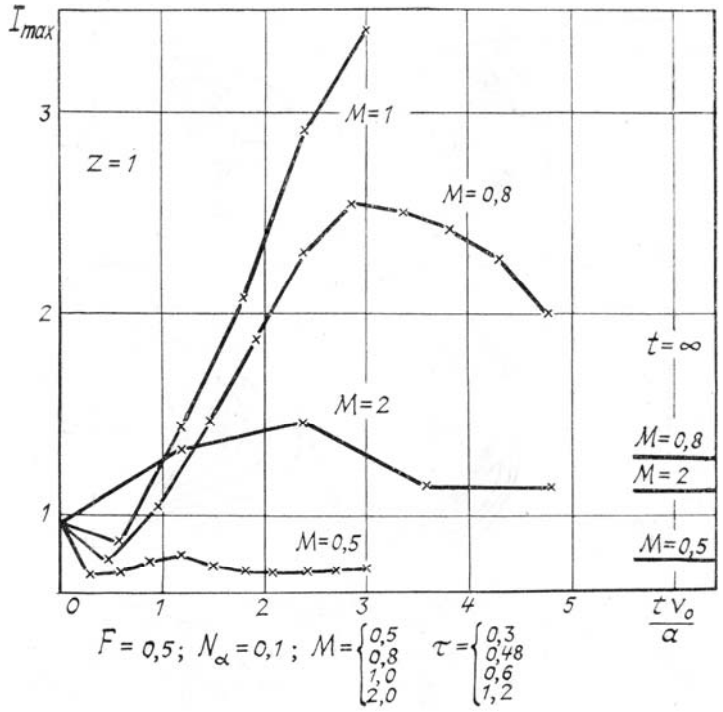

FIG. 2.

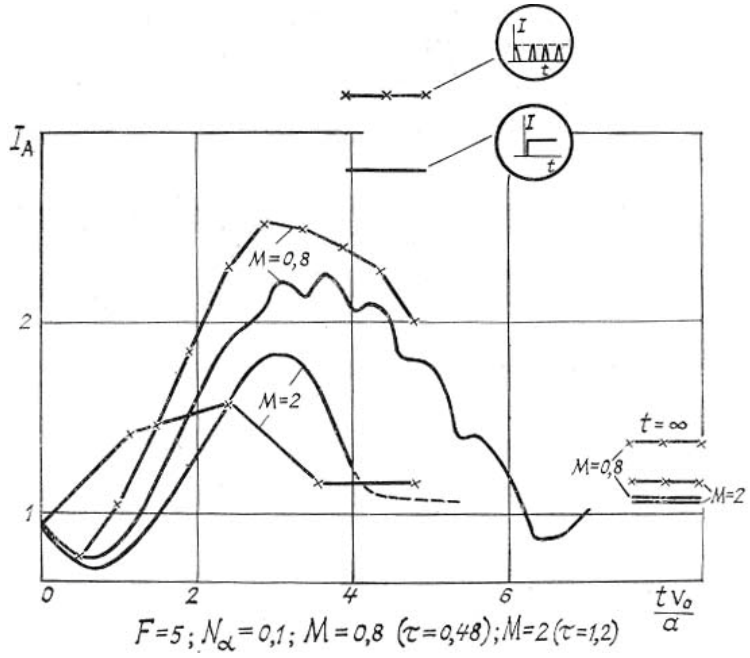

FIG. 3.

Figure 3 shows the peak intensity at the focal cross section $I_A = \max_z\{I_{\max}\}$ as a function of time for the subsonic (M = 0.8) and the supersonic (M = 2) modes. In subsonic flow these curves (likeconstant

density and constant irradiance contours) are similar in behavior, with the peak of the repetitively pulsed radiation exceeding that of the CW radiation for the entirety of the unstabilized thermal blooming process. In the supersonic mode, the peak of the repetitively pulsed radiation is initially higher than that of the CW radiation, but from the time $t_{phys} = 2.3\ \tau_V$ self-focusing of the CW radiation begins to dominate. An analysis has shown that for such combinations of the input parameters ($M = 2$, $F = 5$, $N_\alpha = 0.1$), the chosen period ($\tau = 1.2$) is far from being optimal. The influence of the pulse repetition period (rate) on thermal blooming is generally difficult to investigate. In this paper, we have done so for the investigation has been performed for the quasistationary limit in which Eq. (8) is to be solved only once.

Consider the procedure used for solving the gas dynamics equations in the quasistationary limit of a repetitively pulsed mode of radiation.

Substituting $x' = x - t$, $y' = y$, $t' = t$ in the set of equations (5) and integrating the energy equation, one can obtain a relation between the perturbations of density ρ_1 and pressure P_1 (at least for a single pulse). Taking into account the newly introduced variables, the wave equation for P_1 under the specified initial conditions can be written as

$$\rho_1(x,y,z,t)=M^2P_1(x,y,z,t)-\tau I_1\left[x-(t-t_*),y,z\right]; \quad (11)$$

$$\frac{\partial^2 P_1}{\partial t'^2}-\frac{1}{M^2}\nabla'^2_{\perp}P_1=0;\ P_1|_{t'=t_*}=\frac{\tau}{M^2}I_1(x'+t_*,y',z);$$

$$\left.\frac{\partial P_1}{\partial t'}\right|_{t'=t_*}=0 \quad (12)$$

Here t_* is the emission time for the pulse under consideration. It is convenient to choose it so that at the moment of the blooming n-th pulse emission, the coordinates x' and x coincide, i.e. $t_* = -n\tau$. Summing up the solutions of Eq. (12), i.e. the function $P_1(x', y', z', 0)$, from $n = 1$ to n_{max}, which should be relatively large for the sum to be practically constant, the desired density perturbation ρ_1 can be obtained.

To solve Eq. (12), a Fourier transform technique (discrete Fourier series expansion) over the rather large grid area $-1/2 < x,\ y < +1/2$ should be employed. The relationship between the harmonics of the intensity $I_1(x' - n\tau, y', z)$ and the pressure $P_1(x', y', z, 0)$ functions can be taken from the wave equation. Finally, we obtain

$$I(x'-n\tau,y',z)=\sum_{i=1}^{N_x}\sum_{j=1}^{N_y}A_{ij}(z)\sin\left[\pi i\left(\frac{x'}{l}+\frac{1}{2}\right)\right]\times$$

$$\times\sin\left[\pi j\left(\frac{y'}{2}+\frac{1}{2}\right)\right];$$

$$P_1(x',y',z,0)=\frac{\tau}{M^2}\sum_{i=1}^{N_x}\sum_{j=1}^{N_y}A_{ij}(z)\cos(\omega_{ij}n\tau)\times$$

$$\times\sin\left[\pi i\left(\frac{x'}{l}+\frac{1}{2}\right)\right]\sin\left[\pi j\left(\frac{y'}{l}+\frac{1}{2}\right)\right];$$

$$\omega_{ij}=\left(\frac{\pi}{Ml}\right)^2(i^2+j^2). \quad (13)$$

To economize on computer memory and execution time, we suggest displacing the center of the grid by $n\tau/2$ along the x axis from pulse to pulse. In doing so, the grid area size 1 can be reduced without any deterioration in terms of accuracy. The number of previous pulses which should be taken into consideration to find the perturbed pressure field using Eq. (13) can be determined by assumption that the acoustic wave originating from the region occupied by radiation at the time $t_* = -n\tau$, and having reflected from the boundaries of the grid area, could not reach the region where the radiation is at a time $t = 0$. If the last pulse contribution to the overall sum of the pressure perturbations is sufficiently large, contributions of the following pulses are computed using the approximate formula which may be derived from the known solution[11] of Eq. (12) in the integral form

$$P_1(x',y',z,0)=\frac{M^{-3/2}}{\pi\sqrt{2n\tau}}\int_0^{2\pi\tau/M}\sqrt{\varepsilon}\,\frac{\partial^2 g(\xi(\varepsilon))}{\partial\,\xi^2}\,d\varepsilon-$$

$$-\frac{M^{-1/2}}{\pi(2n\tau)^{3/2}}\int_0^{2\pi\tau/M}\sqrt{\varepsilon}\,\frac{\partial g(\xi(\varepsilon))}{\partial\,\xi}\,d\varepsilon;$$

$$\xi(\varepsilon)=-\varepsilon+x'+n\tau\frac{1-M}{M};\quad g(\xi)=\tau\int_{-\infty}^{+\infty}I_1(\xi,\eta,z)\,d\eta \quad (14)$$

As a result, for the quasistationary limit, the procedure for computing the main term in the density perturbation can be written as follows:

$$\rho_1(x,\ y,\ z)=M^2\sum_{n=1}^{n_{max}}p_{1,n}(x',\ y',\ z)-$$

$$-\tau\sum_{n=1}^{n_{max}}I_1(x'-n\tau,\ y',\ z), \quad (15)$$

where $P_{1,n}$ is calculated using Eq (13) or (15). It should be noted that ρ_1 in the quasistationary limit is actually a periodic function. Equation (15) describes this function at the end of the pulse period, i.e., at the moment the next blooming pulse is emitted for which a solution of Eq. (8) is constructed.

Let us examine the results of the thermal blooming calculations. The general feature of the quasistationary mode is the periodic behavior

of density perturbations in the thermal trace, shown in Fig. 1. In some cases it results in the formation of corresponding local intensity peaks in the thermal trace. Figure 4 shows the peak intensity I_{max} as function of the period τ for three situations: a) $M = 2$, $F = 5$, $N_\alpha = 0.1$; b) $M = 0.8$, $F = 5$, $N_\alpha = 0.1$; c) $M \ll 1$, $F = 5$, $N_\alpha = 0$. The distance $z = 1.2$ along the beam is chosen for calculations close to the focal length in most instances. The purpose of our investigation was to find the periods for which self-focusing was the greatest (for example, near the peak). The minimum values of τ used for calculations are $\tau = 0.25$–0.3. At $\tau = 0$, the peak intensity values obtained in the calculations of stationary thermal CW blooming in the specified gas dynamic modes have been used. The period between pulses $\tau_2 = 1.8\tau_v$ is optimal for the convective mode (c), $\tau_2 = 2\tau_v$ is optimal for the supersonic mode (a) and $\tau_2 \approx 0.6\tau_v$ is optimal for the subsonic mode (b). A substantial decrease of the peak intensity I_{max} as the pulse period increases is due to a peak intensity bifurcation in the subsonic mode.

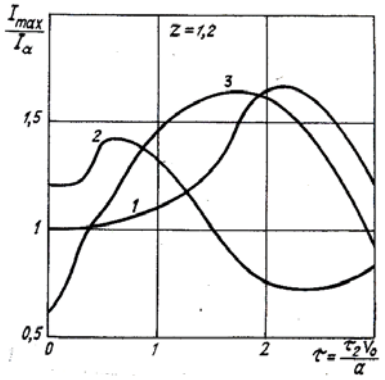

FIG. 4.

In conclusion it should be noted that for the unstabilized state of repetitively pulsed radiation, the thermal blooming effect has an extremum (e.g., at the intensity peak and its vicinity), and the maximum intensity can considerably exceed the initial value as well as the corresponding value for the quasistationary limit. Variation of the period between pulses allows the maximum increase of the intensity peak to be achieved in th'e convective, subsonic and supersonic gas dynamic modes.

REFERENCES

1. V.E. Zuev, *Laser Beam Propagation in the* Atmosphere (Radio i Svjaz, Moscow, 1981).
2. J.M. Strohbehn, *Laser Beam Propagation in the Atmosphere* (N.Y., 1978).
3. V.V. Vorobjev, *Laser Beam Thermal Blooming in the Atmosphere: Theory and the Modeling)* (Nauka, Moscow, 1987).
4. P.B. Ulrich and J. Wallace, J. Opt. Soc. Am., **83**, 8 (1973).
5. J. Wallace and J.Q. Lilly, J. Opt. Soc. Am., **64**, 1651 (1974).
6. J.Q. Lilly and T.Q. Miller, AIAA Journ., **15**, 434 (1977).
7. M.N. Kogan and A.N. Kucherov, Doklady Akad. Nauk SSSR, **251**, 575 (1980).
8. R. Peire and T. Taylor, *Computational Methods in Fluid Mechanics Problems* (Gidrometeoizdat, Leningrad, 1986)
9. Fleck, Morris and Feit, Appl. Phys., **10**, 129 (1976).
10. A.N. Kucherov, Zh. Tekh. Fiz. **52**, 1549 (1982).
11. A.N. Tikhonov and A.A. Samarskii, Equations of Mathematical Physics, (Nauka, Moscow, 1972).